Proceedings of the 5th WSEAS International Conference on Telecommunications and Informatics, Istanbul, Turkey, May 27-29, 2006 (pp515-523)

Representation of Rotational Mechanical Parts by Parametric Equations

ENRIQUE CHICUREL-UZIEL
Instituto de Ingeniería, UNAM
Universidad Nacional Autónoma de México
C. U., Coyoacán, México 04510 D.F.
MÉXICO
http://www.iingen.unam.mx

Abstract:-A systematic procedure to build up the parametric equations of the surface of a rotational mechanical part by Analytical Geometry is proposed. The equations are exact and require no inequalities. 3D Plots are generated from these equations. An example referring to a roller chain sprocket is presented.

Key-Words:-3D Surfaces, Analytic Geometry, Sprocket equation.

1 Introduction

Using Analytic Geometry exclusively, equations and plots were established to represent a polygonal cylinder and the main view of a chain sprocket [1], the former is a 3D plot and the latter a 2D plot. It is only natural to take one further step: the parametric equations and plot of the surface of a 3D chain sprocket and these are presented in this paper. But the development of the equations is quite systematic and applicable to a large class of mechanical rotational elements.

2 Nomenclature

d Roller diameter
D_B Bore diameter
D_H Hub diameter
f Flange thickness
g, h Dimensions of the bevel of the teeth, Fig. 1
L Axial length
P Circular pitch
N Number of teeth
R_C Radial coordinate at the start of the tooth bevel, Fig. 1
r_R Radial coordinate at the bottom of the tooth root
r_T Radial coordinate at the tip of the tooth
α Angular coordinate at the tip of the tooth
θ_C Angular coordinate at the start of the tooth bevel

3 Mathematical Devices

The following mathematical devices will be used to assemble the sprocket equations.

3.1 The Heaviside Unit Step

Cauchy represented his limiting coefficient by the following equation, [2]:

$$H(x,a)=\frac{1}{2}\left(1+\frac{x-a}{|x-a|}\right) \qquad (1)$$

but it turned out that this function is, in fact, the unit step function named after Heaviside much later. Incidentally, for a period of time, the author thought that he had been the first to propose this representation.

3.2 The Function Concatenation Procedure

A composite function [3]:

$$\begin{aligned} f(x) &= f_{12}(x) && a_1 \le x \le a_2 \\ f(x) &= f_{23}(x) && a_2 \le x \le a_3 \\ &\vdots && \vdots \\ f(x) &= f_{n-1,n}(x) && a_{n-1} \le x \le a_n \end{aligned}$$

May be expressed as the single concatenated equation:

$$\begin{aligned} & f(x) = H(x,a_1) f_{12}(x) \\ & + H(x,a_2)\left(- f_{12}(x) + f_{23}(x)\right) + \ldots \\ & + H(x,a_{n-1})\left(- f_{n-2,n-1}(x) + f_{n-1,n}(x)\right) \\ & + H(x,a_n)\left(- f_{n-1,n}(x)\right) \end{aligned}$$

this equation is valid from x = - ∞ to x = + ∞.

3.3 The Reflect and Repeat Function

The reflect and repeat function was proposed in Cartesian form in [4]. The following is the polar form, [1]:.

$$\phi = \left(\frac{1}{N}\right)\arccos[\cos(N\theta)] \qquad (2)$$
$$N = 2\pi / T$$

If in a function $f(\theta)$, θ is replaced by ϕ the resulting function $f(\phi)$ is made up of N identical lobes in the interval $0 \le \theta \le 2\pi$. The first lobe is made up of two symmetrical halves, i.e., the first half is identical to the initial segment of $f(\theta)$ from $\theta = 0$ to $\theta = 0.5\ T$, and the second half is the reflection of the first half with respect to the radius at $\theta = 0.5\ T$.

4 Derivation of the Sprocket Equation

The following development will be presented in detail so as to bring out the systematic approach but, also, to make the paper more readable.

The method to establish the equation is based on the procedure required to generate a plot from it.

In the first place, since this work refers to rotational parts, it seems adequate to use cylindrical coordinates. The plot of the surface is generated by two parameters: s and θ. Parameter s generates the 2D periphery of the radial cross section of the sprocket. The parameter θ rotates this periphery around the axis of the sprocket and, in so doing, generates its surface. As it rotates the form of the periphery varies, i.e., it is a function of θ.

The characteristics of the sprocket are defined by $P, N, d, D_H, D_B, L, f, g$ and h. The quantities P, N and d are used to determine the tooth profile, $r(\theta)$, in accordance to the Appendix. The quantities D_H, D_B, L, f, g and h will be used presently to establish the revolving 2D periphery, Fig.1. The axis of the sprocket coincides with the z axis.

$$R_H = \frac{D_H}{2}; \qquad R_B = \frac{D_B}{2} \qquad (3)$$

From Fig. 1 the following relations are established.

$$\begin{aligned} \mu &= \arctan\left(\frac{g}{h}\right) \\ r_T &= r(\alpha) \\ R_C &= r_T - h \\ u_C &= \frac{f}{2\tan\mu} \\ R_p &= R_C + u_C \\ v &= \frac{f}{2} \\ u &= R_p - r \\ w &= \frac{f}{2} - v \end{aligned} \qquad (4)$$

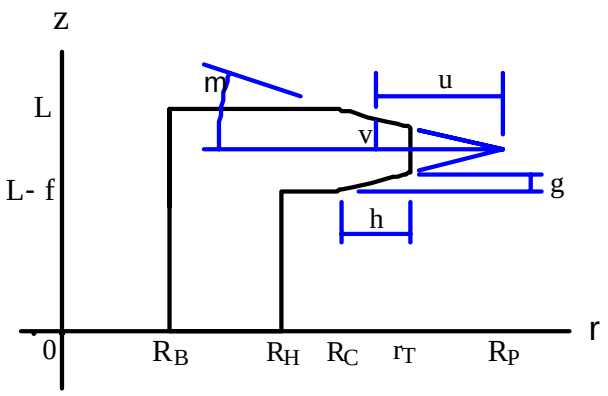

Fig. 1

Fig. 2. shows the two possible typical peripheries of the radial cross section, namely: 0,1,2,3,4a,5a,6a and 0,1,2,3,4b,5b,6b,7b,8b, depending on whether the tooth radial coordinate *r* of the particular cross section is smaller or larger than R_C or equivalently whether the angular coordinate θ is smaller or larger than θ_C.

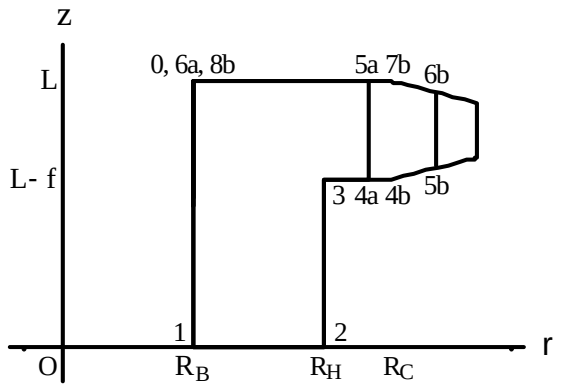

Fig 2

From Fig. 2 the lengths are established of the line segments that make up the revolving periphery:

$$
\begin{aligned}
&L_{01} = L \\
&L_{12} = R_H - R_B \\
&L_{23} = L - f \\
&L_{34a} = r - R_H \\
&L_{4a5a} = f \\
&L_{5a6a} = r - R_B \\
&L_{34b} = R_C - R_H \\
&L_{4b5b} = \frac{w}{\sin\mu} \\
&L_{5b6b} = f - 2w \\
&L_{6b7b} = L_{4b5b} \\
&L_{7b8b} = R_C - R_B
\end{aligned}
\qquad (5)
$$

Using the previous lengths the values of the parameter*s* at the turns of the periphery are established:

$$
\begin{aligned}
&s_0 = 0 \\
&s_1 = s_0 + L_{01} \\
&s_2 = s_1 + L_{12} \\
&s_3 = s_2 + L_{23} \\
&s_{4a} = s_3 + L_{34a} \\
&s_{5a} = s_{4a} + L_{4a5a} \\
&s_{6a} = s_{5a} + L_{5a6a} \\
&s_{4b} = s_3 + L_{34b} \\
&s_{5b} = s_{4b} + L_{4b5b} \\
&s_{6b} = s_{5b} + L_{5b6b} \\
&s_{7b} = s_{6b} + L_{6b7b} \\
&s_{8b} = s_{7b} + L_{7b8b}
\end{aligned}
\qquad (6)
$$

The radius of the various segments of the rotating periphery are now expressed in terms of the parameter *s*:

$$
\begin{aligned}
&\rho_{01} = R_B \\
&\rho_{12} = R_B + s - s_1 \\
&\rho_{23} = R_H \\
&\rho_{34} = \rho_{34a} = \rho_{34b} = R_H + s - s_3 \\
&\rho_{4a5a} = r \\
&\rho_{5a6a} = r - (s - s_{5a}) \\
&\rho_{4b5b} = R_C + (s - s_{4b})\cos\mu \\
&\rho_{5b6b} = r \\
&\rho_{6b7b} = r - (s - s_{6b})\cos\mu \\
&\rho_{7b8b} = R_C - (s - s_{7b})
\end{aligned}
\qquad (8)
$$

The various segments of the "*a* " circuit are now concatenated:

$$
\begin{aligned}
\rho_{04}(s) = {} & H(s,s_0)\rho_{01} + H(s,s_1)(-\rho_{01} + \rho_{12}) \\
& + H(s,s_2)(-\rho_{12} + \rho_{23}) + H(s,s_3)(-\rho_{23} + \rho_{34})
\end{aligned}
\qquad (9)
$$

$$
\begin{aligned}
\rho_{4a6a}(s,r) = {} & \rho_{4a5a} + H(s,s_{5a})(-\rho_{4a5a} + \rho_{5a6a}) \\
& + H(s,s_{6a})(-\rho_{5a6a})
\end{aligned}
\qquad (10)
$$

Thus the equation for radius of any point in the " *a* " circuit is:

$$\rho_a(s,r) = \rho_{04} + H(s,s_{4a})(-\rho_{04} + \rho_{4a6a}) \qquad (11)$$

A similar process is carried out in connection with the " *b* " circuit:

$$\rho_{4b8b}(s,r) = \rho_{4b5b} + H(s,s_{5b})(-\rho_{4b5b} + \rho_{5b6b}) + H(s,s_{6b})(-\rho_{5b6b} + \rho_{6b7b}) + H(s,s_{7b})(-\rho_{6b7b} + \rho_{7b8b}) + H(s,s_{8b})(-\rho_{7b8b}) \quad (12)$$

$$\rho_b(s,r) = \rho_{04} + H(s,s_{4b})(-\rho_{04} + \rho_{4b8b}) \quad (13)$$

Thus the general expression of the radius of the revolving periphery is:

$$\rho(s,r) = \rho_a + H(r,r_C)(-\rho_a + \rho_b) \quad (14)$$

Proceeding in an analogous manner in connection with the *z* coordinates:

$$\begin{aligned} z_{01} &= L - (s - s_0) \\ z_{12} &= 0 \\ z_{23} &= s - s_2 \\ z_{34} &= z_{34a} = z_{34b} = L - f \\ z_{4a5a} &= L - f + s - s_{4a} \\ z_{5a6a} &= L \\ z_{4b5b} &= L - f + (s - s_{4b})\sin\mu \\ z_{5b6b} &= L - f + w + s - s_{5b} \\ z_{7b8b} &= L \end{aligned} \quad (15)$$

$$z_{04}(s) = H(s,s_0)z_{01} + H(s,s_1)(-z_{01} + z_{12}) + H(s,s_2)(-z_{12} + z_{23}) + H(s,s_3)(-z_{23} + z_{34}) \quad (16)$$

$$z_{4a6a}(s,\theta) = z_{4a5a} + H(s,s_{5a})(-z_{4a5a} + z_{5a6a}) + H(s,s_{6a})(-z_{5a6a}) \quad (17)$$

$$z_a(s,r) = z_{04} + H(s,s_{4b})(-z_{04} + z_{4a6a}) \quad (18)$$

$$z_{4b8b}(s,\theta) = z_{4b5b} + H(s,s_{5b})(-z_{4b5b} + z_{5b6b}) + H(s,s_{6b})(-z_{5b6b} + z_{6b7b}) + H(s,s_{7b})(-z_{6b7b} + z_{7b8b}) + H(s,s_{8b})(-z_{7b8b}) \quad (19)$$

$$z_b(s,r) = z_{04} + H(s,s_{4b})(-z_{04} + z_{4b8b}) \quad (20)$$

and thus the z coordinate at any point of the revolving periphery is:

$$z(s,\theta) = z_a + H(\theta,\theta_C)(-z_a + z_b) \quad (21)$$

Replacing θ by the polar reflect and repeat function ϕ, the polar parametric equations of the sprocket are obtained:

$$\rho = \rho(s,\phi) \qquad z = z(s,\phi) \quad (22)$$

or in Cartesian coordinates:

$$x = \rho(s,\phi)\cos\theta \qquad y = \rho(s,\phi)\sin\theta \qquad z = z(s,\phi) \quad (23)$$

It is worth noticing that the last terms of Eqs. (10),(12),(17) and (19) have, respectively, the same effects as the following inequalities:

$$\begin{aligned} \rho_{4a6a} &= 0 \qquad s > s_{6a} \\ \rho_{4b8b} &= 0 \qquad s > s_{8b} \\ z_{4a6a} &= 0 \qquad s > s_{6a} \\ z_{4b8b} &= 0 \qquad s > s_{8b} \end{aligned} \quad (24)$$

These effects carry over to Eqs. (11), (13),(18) and (20) so that they have, respectively, the same effects as the following inequalities:

$$\begin{aligned} \rho_a &= 0 \qquad s > s_{6a} \\ \rho_b &= 0 \qquad s > s_{8b} \\ z_a &= 0 \qquad s > s_{6a} \\ z_{8b} &= 0 \qquad s > s_{8b}: \end{aligned} \quad (25)$$

Furthermore, these effects also carry over to Eqs. (14) and (21) so that they have the same effect as the following inequality:

$$\left.\begin{aligned} \rho &= 0 \\ z &= 0 \end{aligned}\right\} \qquad s > s_{8b} \quad (26)$$

But, it must be emphasized, that all these effects are already contained in Eqs. (10) to (14) and (17) to (21) thus neither inequalities (24) to (26), nor any other inequality, are part of the sprocket equations (22) or (23).

Eq. (26) establishes the point at which s stops to generate a surface.

5 Example: a Specific Sprocket

The parametric equations of an ASA, No.80 sprocket with 13 teeth will be established.
The following are the teeth characteristics, [5]:

$$\begin{aligned} N &= 13 \\ P &= 1'' \quad = 2.54\ cm \\ d &= 0.625'' \quad = 1.5875\ cm \end{aligned} \qquad (27)$$

The following are the sprocket dimensions,[6]:

$$\begin{aligned} D_H &= 3.03125'' \quad = 7.699375\ cm \\ D_B &= 1.5 \quad = 3.81\ cm \\ L &= 1.5625 \quad = 3.96875\ cm \\ f &= 0.575 \quad = 1.4605\ cm \\ h &= 0.5 \quad = 1.27\ cm \\ g &= 0.125 \quad = 0.3175\ cm \end{aligned} \qquad (28)$$

Numerical values (27) are substituted in the equations of the Appendix and the resulting equation (A2) of the tooth profile as well as values (28) are substituted into equations (3) to (23) and thus the parametric equations (22) and (23) of the sprocket are obtained.

5.1 Rendering of the Sprocket 3D Plot

Attempts to obtain the sprocket equations and plot were made by use of *Mathematica, Maple* and *Matlab*, but only the attempt by use of *Mathematica* was successful (this may be partly due to the author´s greater familiarity with the plotting procedures of this software) and it is the one presented here.

Now, both in the concept of the unit step and in Eq. (1) its magnitude at the "jump" is undefined. Nonetheless, plotting Eq. (1) in *Mathematica*, Fig.1, leaves a spurious vertical trace which is not the case if *Matlab* is used, Fig. 2. In *Maple* the user may determine whether this trace appears or not.

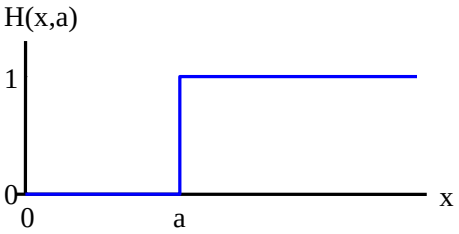

Fig. 3

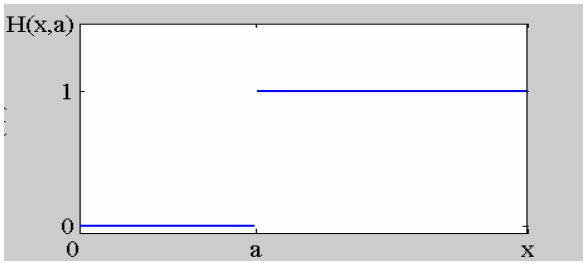

Fig. 4

It is convenient to plot Eqs. (11), (13), (18) and (20). Substituting the value of $\theta = \theta_R = 0$ at the bottom of the root of the tooth as well as the value $\theta = \theta_T = \alpha = 0.24166$, (Eq. A1 of the Appendix) each in turn into Eq. (A2) of the appendix, yield the extreme values of the tooth radius:

$$r_R = 4.50508\ cm \qquad (29)$$

$$r_T = 6.08871\ cm \qquad (30)$$

Substituting values (29) into Eqs. (11) and (18) yield

$$\rho_a(s, r_R) = \rho_{aR} \qquad (31)$$

$$z_a(s, r_R) = z_{aR} \qquad (32)$$

Substituting values (30) into Eqs. (13) and (20) yield

$$\rho_b(s, r_T) = \rho_{bT} \qquad (33)$$

$$z_b(s, r_T) = z_{bT} \qquad (34)$$

Fig. 5 are the superimposed plots of Eqs. (31) and (33) and Fig. 6 are the superimposed plots of Eqs. (32) and (34).

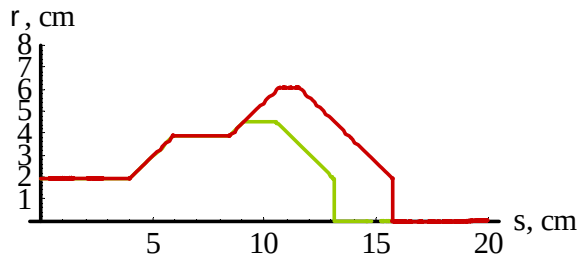

Fig. 5

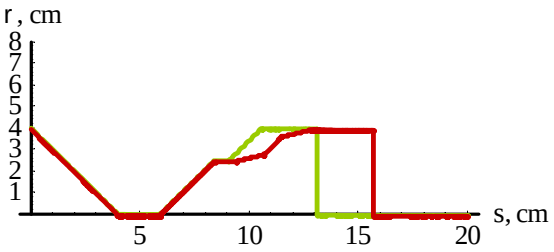

Fig. 6

The use of *Mathematica* in this work has resulted in the two spurious vertical traces at the end of the plots of Figs. 5 and 6. A plot of z from Eq. (14) vs. ρ of equation from Eq. (21) for any specific value of θ yields the radial cross section for that value similar to Fig. 2 but with a spurious line trace going from point 8b to the origin. Thus a 3D parametric plot of equations (22) or (23) yields the sprocket surface with a spurious cone inside its bore.

In order eliminate all of these spurious traces, instead of prescribing a stop of the parameter s at points 6a and 8b, Fig. 2 , a partial retracing of the bore may be prescribed by adding the following elements:

$$\rho_{6a7a} = R_B$$
$$\rho_{8b9b} = R_B$$
$$z_{6a7a} = L - (s - s_{6a})$$
$$z_{8b9b} = L - (s - s_{8b}) \qquad (35)$$

Using the previous equations, Eqs. (10) to (14), (17) to (21) respectively are modified thus:

$$\rho_{4a6aM} = \rho_{4a6a} + H(s, s_{6a})\rho_{6a7a} \qquad (36)$$
$$\rho_{aM} = \rho_{04} + H(s, s_{4a})(-\rho_{04} + \rho_{4a6aM}) \qquad (37)$$
$$\rho_{4b8bM} = \rho_{4b8b} + H(s, s_{8b})\rho_{8b9b} \qquad (38)$$
$$\rho_{bM} = \rho_{04} + H(s, s_{4b})(-\rho_{04} + \rho_{4b8bM}) \qquad (39)$$
$$\rho_M = \rho_{aM} + H(r, R_C)(-\rho_{aM} + \rho_{bM}) \qquad (40)$$

$$z_{4a6aM} = z_{4a6a} + H(s, s_{6a})z_{6a7a} \qquad (41)$$
$$z_{aM} = z_{04} + H(s, s_{4a})(-z_{04} + z_{4a6aM}) \qquad (42)$$
$$z_{4b8bM} = z_{4b8b} + H(s, s_{8b})z_{8b9b} \qquad (43)$$
$$z_{bM} = z_{04} + H(s, s_{4b})(-z_{04} + z_{4b8bM}) \qquad (44)$$
$$z_M = z_{aM} + H(r, R_C)(-z_{aM} + z_{bM}) \qquad (45)$$

Fig. 7 shows the superimposed plots of Eqs. (37) and (39) and Fig. 8 shows the superimposed plots of Eqs. (42) and (44). Figs. 1 and 2 are each the parametric plot of z_M, Eq. (45) vs. ρ_M, Eq. (40).

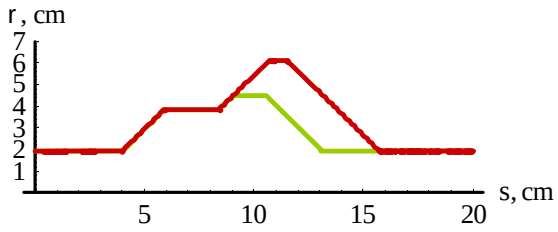

Fig. 7

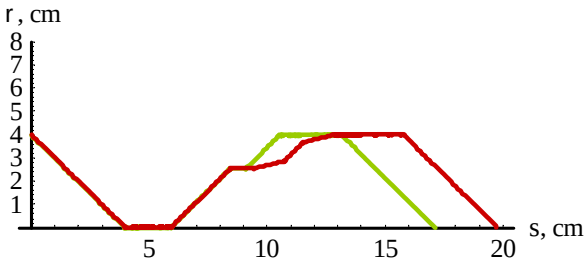

Fig. 8

Fig. 9 is the parametric plot of the following equations:

$$x_M = \rho_M(s, \phi)\cos\theta$$
$$y_M = \rho_M(s, \phi)\sin\theta$$
$$z_M = z_M(s, \phi) \qquad (46)$$

An odd number of teeth was deliberately chosen to show that the figure need not be symmetrical as can be appreciated in Fig. 9. To obtain a reasonably defined image it was necessary to specify a large number, 650, of plot points. This, in turn required a very large image because otherwise it would have been either very dark or reduced to a mere silhouette.

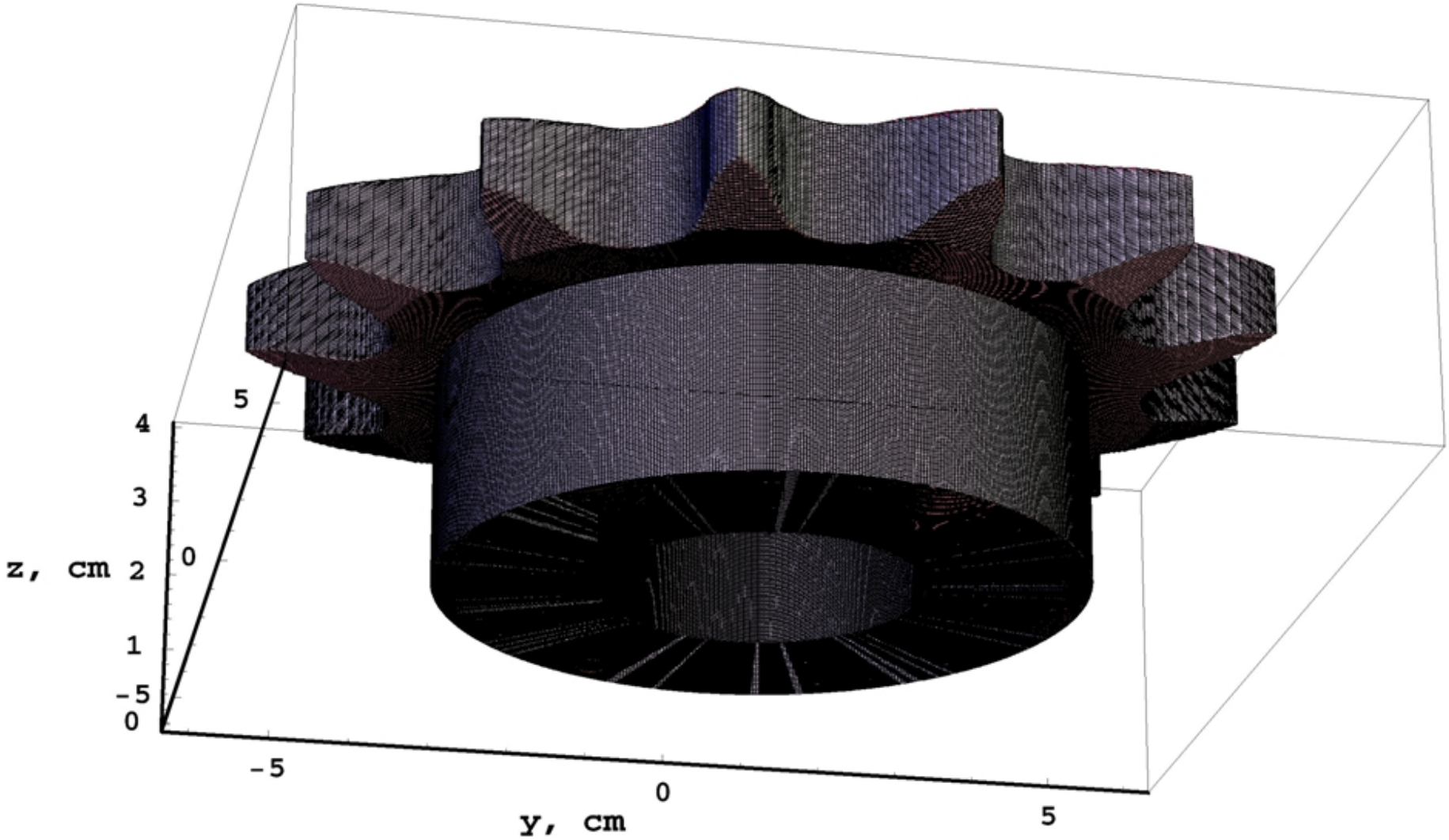

Fig. 9

6 Discussion and Conclusions

It has been shown that it is possible to obtain the parametric equations of the surface of a relatively complex quasi radially symmetric object by the exclusive use of Analytic Geometry expressed in simple algebraic terms.

The representation did not include details such as a keyway or a fillet radius but it is easy to see that these would pose no big problem.

Although *Mathematica* proved to be very adequate for this purpose, the fact that the graphs containing a discontinuity produce a spurious trace required the equations to be slightly modified for plotting. Since neither *Matlab* nor *Maple* leave such a trace, it is only natural to speculate that if the plots of such objects are ever obtained by use of these softwares it will be from the unmodified equations.

It is pertinent to point out that the equations obtained are not unique. A different set of parametric equations would be obtained if the periphery of the *transverse*, and not the radial, cross section of the sprocket was used to sweep the surface as it is displaced in the axial direction.

The author hopes that the surface equations obtained will lead to useful applications.

Acknowledgments

The author wishes to express his appreciation of the valuable assistance of Javier Hernández, María de Jesús Ortega, Pedro Osnaya, Carlos Becerra, Fernando Maldonado and Aldo Ramírez of the Computer Sevices Section of our Institute

Appendix

According to the ANSI standards the profile of the tooth of the sprocket is made of three circle arcs and a straight line segment, Fig. A1, [5]. The axis of the sprocket lies at the origin (not shown) to the left of the figure.

The arcs have centers at points O_i with coordinates (x_{Oi}, y_{Oi}) and radii R_i, they start at points P_i with coordinates x_{Pi}, y_{Pi} and θ_{Pi} and end at points P_{i+1} where $I = 1,\ 2,\ 4$. The straight line segment goes from point P_3 to point P_4. The following relations define these quantities in terms of the specifications P, N and d. The full profile of one half tooth is the curve $P_1P_2P_3P_4P_5$, [5], [1].

$$R_1 = 0.5025d + 0.0015$$

$$\alpha = \frac{\pi}{N} \qquad \text{(A1)}$$

$$\beta = \frac{\pi}{180}\left(35 + \frac{60}{N}\right)$$

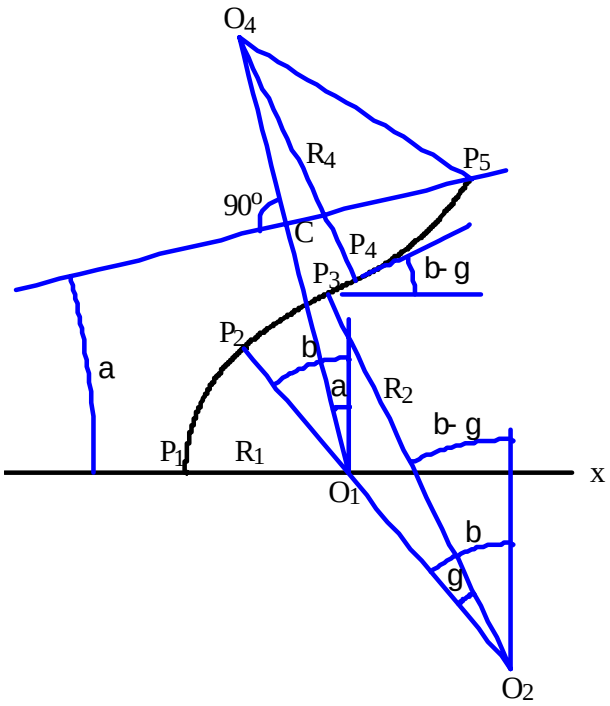

Fig. A1

$$\gamma = \frac{\pi}{180}\left(18 - \frac{56}{N}\right)$$

$$D = \frac{P}{sin\ \alpha}; \qquad x_{01} = \frac{D}{2}; \qquad y_{01} = 0$$

$$x_{P1} = \frac{1}{2}(D-d); \qquad y_{P1} = 0; \qquad \theta_{P1} = 0$$

$$x_{02} = \frac{D}{2} + 0.8\ d\ \sin\beta$$
$$y_{02} = -0.8\ d\ \cos\beta$$

$$x_{P2} = \frac{D}{2} - R_1\ \sin\beta; \qquad y_{P2} = R_1\ \cos\beta$$

$$\theta_{P2} = \arctan\frac{y_{P2}}{x_{P2}}$$

$$R_2 = R_1 + 0.8\ d$$

$$x_{P3} = x_{O2} - R_2 \sin(\beta-\gamma)$$
$$y_{P3} = y_{O2} + R_2 \cos(\beta-\gamma)$$
$$\theta_{P3} = \arctan\frac{y_{P3}}{x_{P3}}$$

$$x_{04} = 0.5\ D - 1.4\ d\ \sin\alpha; \qquad y_{04} = 1.4\ d\ \cos\alpha$$

$$m_a = \tan(\beta-\gamma); \qquad b_a = y_{P3} - m_a x_{P3}$$
$$m_b = \tan(\beta-\gamma+0.5\ \pi); \qquad b_b = y_{04} - m_b x_{04}$$

$$x_{P4} = \frac{b_b - b_a}{m_a - m_b}; \qquad y_{P4} = m_b x_{P4} + b_b$$
$$\theta_{P4} = \arctan\frac{y_{P4}}{x_{P4}}$$

$$R_4 = \sqrt{(x_{P4}-x_{04})^2 + (y_{P4}-y_{04})^2}$$

The following are the polar equations of the arcs:

$$r_{12}(\theta) = x_{01}\ \cos\theta + y_{01}\ \sin\theta - \sqrt{\left(x_{01}\ \cos\theta + y_{01}\ \sin\theta\right)^2 - \left({x_{01}}^2 + {y_{01}}^2 - {R_1}^2\right)}$$

$$r_{23}(\theta) = x_{02}\ \cos\theta + y_{02}\ \sin\theta - \sqrt{\left(x_{02}\ \cos\theta + y_{02}\ \sin\theta\right)^2 - \left({x_{02}}^2 + {y_{02}}^2 - {R_2}^2\right)}$$

$$r_{45}(\theta) = x_{04}\ \cos\theta + y_{04}\ \sin\theta + \sqrt{\left(x_{04}\ \cos\theta + y_{04}\ \sin\theta\right)^2 - \left({x_{04}}^2 + {y_{04}}^2 - {R_4}^2\right)}$$

The equation of the straight line segment is:

$$r_{34}(\theta) = \frac{b_a}{\sin\theta - m_a\ \cos\theta}$$

Concatenating the four previous equations the tooth profile equation is obtained, thus:

$$r\ (\theta) = r_{12}(\theta) + H(\theta,\theta_{P2})\{-r_{12}(\theta) + r_{23}(\theta)\} + H(\theta,\theta_{P3})\{-r_{23}(\theta) + r_{34}(\theta)\} + H(\theta,\theta_{P4})\{-r_{34}(\theta) + r_{45}(\theta)\} \qquad \text{(A2)}$$

References:

[1] Chicurel-Uziel, E., Single Equation Without Inequalities to Represent a Composite Curve, *Computer-aided geometric design,* Vol. 21, No.1, 2003/2004, pp. 23-42.

[2] Hoskins, R. F., *Generalized functions*, Ellis Horwood Ltd., Wiley, 1979, p 42.

[3] Chicurel-Uziel, E., Non-piecewise Representation of Discontinuous Functions and its Application to the Clebsch Method for Beam Deflections, *Meccanica***,** Vol.34, No.4, 1999-2000, pp. 281 -285.

[4] Chicurel-Uziel, E., Exact, Single Equation, Closed Form Solution of Vibrating Systems with Piecewise Linear Springs, *Journal of Sound and Vibration*, Vol. 245, No 2 , 2001, pp.285-301.

[5] Oberg, E. et al, Machinery´s Handbook, 23rd Ed., Industrial Press Inc., 1988,. p. 2301.

[6] *Dodge Engineering Catalog*, Reliance Electric, 1993, 1.1R, p. D11-24.